

Chapman University

## Chapman University Digital Commons

---

Biology, Chemistry, and Environmental Sciences  
Faculty Articles and Research

Science and Technology Faculty Articles and  
Research

---

7-13-2021

### **An Integrative Model for Soil Biogeochemistry and Methane Processes: I. Model Structure and Sensitivity Analysis**

Daniel M. Ricciuto

Xiaofeng Xu

Xiaoying Shi

Yihui Wang

Xia Song

*See next page for additional authors*

Follow this and additional works at: [https://digitalcommons.chapman.edu/sees\\_articles](https://digitalcommons.chapman.edu/sees_articles)



Part of the Atmospheric Sciences Commons, Biogeochemistry Commons, Climate Commons, Environmental Health and Protection Commons, Environmental Indicators and Impact Assessment Commons, Environmental Monitoring Commons, Other Environmental Sciences Commons, and the Soil Science Commons

---

---

# An Integrative Model for Soil Biogeochemistry and Methane Processes: I. Model Structure and Sensitivity Analysis

## Comments

This article was originally published in *Journal of Geophysical Research: Biogeosciences*, volume 126, in 2021. <https://doi.org/10.1029/2019JG005468>

## Creative Commons License



This work is licensed under a [Creative Commons Attribution-Noncommercial 4.0 License](https://creativecommons.org/licenses/by-nc/4.0/)

## Copyright

The authors

## Authors

Daniel M. Ricciuto, Xiaofeng Xu, Xiaoying Shi, Yihui Wang, Xia Song, Christopher W. Schadt, Natalie A. Griffiths, Jiafu Mao, Jeffrey M. Warren, Peter E. Thornton, Jeff Chanton, Jason K. Keller, Scott D. Bridgham, Jessica Gutknecht, Stephen D. Sebestyen, Adrien Finzi, Randall Kolka, and Paul J. Hanson



## RESEARCH ARTICLE

10.1029/2019JG005468

This article is a companion to Yuan et al. (2021), <https://doi.org/10.1029/2020JG005963>.

### Key Points:

- A new CH<sub>4</sub> module was integrated into an Earth system model to predict CH<sub>4</sub> fluxes in a northern Minnesota peatland
- The model accurately predicts the seasonal cycle of methane production and net fluxes
- CH<sub>4</sub> substrate and production were the most critical mechanisms regulating temporal patterns of CH<sub>4</sub> fluxes

### Supporting Information:

Supporting Information may be found in the online version of this article.

### Correspondence to:

D. M. Ricciuto,  
[ricciutodm@ornl.gov](mailto:ricciutodm@ornl.gov)

### Citation:

Ricciuto, D. M., Xu, X., Shi, X., Wang, Y., Song, X., Schadt, C. W., et al. (2021). An integrative model for soil biogeochemistry and methane processes: I. Model structure and sensitivity analysis. *Journal of Geophysical Research: Biogeosciences*, 126, e2019JG005468. <https://doi.org/10.1029/2019JG005468>

Received 20 SEP 2019  
 Accepted 4 AUG 2020

### Author Contributions:

**Conceptualization:** Daniel M. Ricciuto, Xiaofeng Xu, Xiaoying Shi, Peter E. Thornton, Paul J. Hanson  
**Data curation:** Christopher W. Schadt, Natalie A. Griffiths, Jeffrey M. Warren, Jeff Chanton, Jason K. Keller, Scott D. Bridgham, Jessica Gutknecht, Stephen D. Sebestyen, Adrien Finzi, Randall Kolka, Paul J. Hanson

© 2021. The Authors.

This is an open access article under the terms of the [Creative Commons Attribution-NonCommercial License](https://creativecommons.org/licenses/by-nc/4.0/), which permits use, distribution and reproduction in any medium, provided the original work is properly cited and is not used for commercial purposes.

# An Integrative Model for Soil Biogeochemistry and Methane Processes: I. Model Structure and Sensitivity Analysis

Daniel M. Ricciuto<sup>1</sup> , Xiaofeng Xu<sup>2</sup> , Xiaoying Shi<sup>1</sup>, Yihui Wang<sup>2</sup>, Xia Song<sup>2</sup>, Christopher W. Schadt<sup>1</sup> , Natalie A. Griffiths<sup>1</sup> , Jiafu Mao<sup>1</sup> , Jeffrey M. Warren<sup>1</sup> , Peter E. Thornton<sup>1</sup> , Jeff Chanton<sup>3</sup> , Jason K. Keller<sup>4</sup>, Scott D. Bridgham<sup>5</sup>, Jessica Gutknecht<sup>6</sup>, Stephen D. Sebestyen<sup>7</sup> , Adrien Finzi<sup>8</sup> , Randall Kolka<sup>7</sup> , and Paul J. Hanson<sup>1</sup> 

<sup>1</sup>Environmental Sciences Division and Climate Change Sciences Institute, Oak Ridge National Laboratory, Oak Ridge, TN, USA, <sup>2</sup>Department Biology, San Diego State University, San Diego, CA, USA, <sup>3</sup>Earth, Ocean, and Atmospheric Sciences, Florida State University, Tallahassee, FL, USA, <sup>4</sup>Schmid College of Science and Technology, Chapman University, Orange, CA, USA, <sup>5</sup>Institute of Ecology and Evolution, University of Oregon, Eugene, OR, USA, <sup>6</sup>Department of Soil, Water, and Climate, University of Minnesota, St Paul, MN, USA, <sup>7</sup>USDA Forest Service Northern Research Station, Grand Rapids, MN, USA, <sup>8</sup>Department of Biology and PhD Program in Biogeoscience, Boston University, Boston, MA, USA

**Abstract** Environmental changes are anticipated to generate substantial impacts on carbon cycling in peatlands, affecting terrestrial-climate feedbacks. Understanding how peatland methane (CH<sub>4</sub>) fluxes respond to these changing environments is critical for predicting the magnitude of feedbacks from peatlands to global climate change. To improve predictions of CH<sub>4</sub> fluxes in response to changes such as elevated atmospheric CO<sub>2</sub> concentrations and warming, it is essential for Earth system models to include increased realism to simulate CH<sub>4</sub> processes in a more mechanistic way. To address this need, we incorporated a new microbial-functional group-based CH<sub>4</sub> module into the Energy Exascale Earth System land model (ELM) and tested it with multiple observational data sets at an ombrotrophic peatland bog in northern Minnesota. The model is able to simulate observed land surface CH<sub>4</sub> fluxes and fundamental mechanisms contributing to these throughout the soil profile. The model reproduced the observed vertical distributions of dissolved organic carbon and acetate concentrations. The seasonality of acetoclastic and hydrogenotrophic methanogenesis—two key processes for CH<sub>4</sub> production—and CH<sub>4</sub> concentration along the soil profile were accurately simulated. Meanwhile, the model estimated that plant-mediated transport, diffusion, and ebullition contributed to ~23.5%, 15.0%, and 61.5% of CH<sub>4</sub> transport, respectively. A parameter sensitivity analysis showed that CH<sub>4</sub> substrate and CH<sub>4</sub> production were the most critical mechanisms regulating temporal patterns of surface CH<sub>4</sub> fluxes both under ambient conditions and warming treatments. This knowledge will be used to improve Earth system model predictions of these high-carbon ecosystems from plot to regional scales.

## 1. Introduction

Northern peatlands contain a vast pool of soil carbon that may be vulnerable to atmospheric release under changing environmental conditions, potentially causing a positive feedback to the climate system (Frolking et al., 2011; Nichols & Peteet, 2019; Yu, 2012). The magnitude of carbon emissions and their mechanistic responses to changing environments are elusive due to the complexity of hydrologic and biogeochemical processes in peatland systems (Blodau, 2002). Methane (CH<sub>4</sub>) is one of the key carbon forms leaving peatlands under anaerobic conditions. Given the high radiative warming potential of CH<sub>4</sub> compared to CO<sub>2</sub> (Neubauer & Magonigal, 2015), it is critically important to accurately predict future CH<sub>4</sub> emissions from global peatlands. Peatlands are typically formed over millennial timescales due to organic carbon inputs, long-term water saturation and low temperatures and thus store major amounts of terrestrial carbon (Yu, 2012). It is expected that hydrological and biogeochemical dynamics play important roles affecting CH<sub>4</sub> fluxes from peatlands, but many of these key processes are missing in current Earth system models (Bohn et al., 2015). Therefore, to build a better predictive capacity for CH<sub>4</sub> dynamics in peatlands, it is necessary to fully consider the processes and environmental conditions controlling CH<sub>4</sub> processes, particularly the

**Formal analysis:** Daniel M. Ricciuto, Xiaofeng Xu, Yihui Wang, Xia Song  
**Funding acquisition:** Paul J. Hanson  
**Investigation:** Daniel M. Ricciuto, Xiaofeng Xu, Jiafu Mao, Paul J. Hanson  
**Methodology:** Daniel M. Ricciuto, Xiaofeng Xu, Xiaoying Shi, Stephen D. Sebestyen, Paul J. Hanson  
**Project Administration:** Randall Kolka, Paul J. Hanson  
**Resources:** Daniel M. Ricciuto, Peter E. Thornton, Paul J. Hanson  
**Software:** Daniel M. Ricciuto, Xiaofeng Xu, Xiaoying Shi  
**Supervision:** Daniel M. Ricciuto, Peter E. Thornton, Paul J. Hanson  
**Validation:** Daniel M. Ricciuto, Xiaofeng Xu, Xia Song, Scott D. Bridgham  
**Visualization:** Daniel M. Ricciuto, Xiaofeng Xu  
**Writing – original draft:** Daniel M. Ricciuto, Xiaofeng Xu  
**Writing – review & editing:** Daniel M. Ricciuto, Xiaofeng Xu, Xiaoying Shi, Yihui Wang, Christopher W. Schadt, Natalie A. Griffiths, Jiafu Mao, Jeffrey M. Warren, Peter E. Thornton, Jeff Chanton, Jason K. Keller, Scott D. Bridgham, Jessica Gutknecht, Stephen D. Sebestyen, Randall Kolka, Paul J. Hanson

vertical dynamics of CH<sub>4</sub> substrates, CH<sub>4</sub> production and oxidation, and the CH<sub>4</sub> transport pathways (Xu et al., 2016).

A recent rise in global atmospheric CH<sub>4</sub> concentrations has been attributed to a number of natural and anthropogenic causes, including emissions from peatlands (Nisbet et al., 2019; Poulter et al., 2017; Rigby et al., 2008). While northern peatlands are thought to contribute less than tropical wetlands and anthropogenic sources currently, boreal wetlands have received recent attention in the modeling community due to their larger area, higher warming rates, and high carbon stocks (Bohn et al., 2015). Model predictions in such studies are highly variable, and simple models based on environmental drivers alone (e.g., temperature and water-table height) have relatively poor predictive skill in predicting CH<sub>4</sub> fluxes across a range of ecosystems (Turetsky et al., 2014). Major uncertainties and model biases likely result from poor model representations of CH<sub>4</sub> production, consumption and transport, and a relatively small number of observations for model validation (Bridgham et al., 2013). Uncertainty in the temperature sensitivity of CH<sub>4</sub> production also contributes to prediction uncertainty at regional to global scales (Riley et al., 2011).

The Spruce and Peatland Responses Under Changing Environments (SPRUCE) experiment presents a unique opportunity to test model responses against observations under experimentally manipulated environmental conditions at an unprecedented scale within a peatland ecosystem. Specifically, SPRUCE is an experiment in an ombrotrophic bog in northern Minnesota designed to assess the response of northern forested peatland ecosystems to increases in temperature and exposure to elevated atmospheric CO<sub>2</sub> concentrations (Hanson et al., 2016, 2017). The SPRUCE project was designed with a primary objective of providing information and data for model development and improvement. Both direct and indirect effects of these experimental perturbations have already been used to develop and refine new peatland modules within Earth system models (Hanson et al., 2017). In this study, we introduce a new model that integrates multiple sources of pre-treatment SPRUCE data about soil biogeochemistry and CH<sub>4</sub> processes (Xu et al., 2014, 2015) into a process-based model. The model is further used to answer the following questions:

1. Can our process-based model framework capture pre-treatment observations of CH<sub>4</sub> fluxes, CH<sub>4</sub> concentrations, and associated biogeochemical data within the level of observation uncertainty?
2. Which model parameters and process drive model prediction uncertainty?
3. What pathways dominate CH<sub>4</sub> emissions?

To answer these questions, we developed a new model structure and compare the model results with field-scale observational data. A model parameter sensitivity analysis was used to further examine the behavior of the new model and the most critical parameters and processes contributing to variations in surface CH<sub>4</sub> fluxes under pre-treatment conditions.

## 2. Methods

### 2.1. Experimental Site and Data Products

The SPRUCE experiment evaluates the response of the existing peatland biological communities to whole-ecosystem warming up to +9°C at both ambient and elevated (~900 ppm) CO<sub>2</sub> concentrations using open-top enclosures (Hanson et al., 2017). These enclosures are located in a *Picea*—*Sphagnum* spp. bog (S1 bog) in northern Minnesota, 40 km north of Grand Rapids (47°30.476' N; 93°27.162' W; 418 m above mean sea level), in the USDA Forest Service Marcell Experimental Forest (Kolka et al., 2011). The S1 bog is an ombrotrophic peatland with a perched water table that has no groundwater inflow, and it is located at the southern margin of the boreal forest in a sub-boreal climate. It is dominated by a mixed black spruce (*Picea mariana*) and larch forest canopy (*Larix laricina*) with various understory shrubs, including Labrador tea (*Rhododendron groenlandicum*), leatherleaf (*Chamaedaphne calyculata*) and blueberry (*Vaccinium* spp.). Annual precipitation and air temperature average 768 mm and 3.3°C respectively (Sebestyen et al., 2011). The S1 bog was harvested in strip cuts in 1969 and 1974 to test the effects of seeding on the natural regeneration of black spruce (Sebestyen et al., 2011). Ground layer vegetation within the S1 bog is composed of a bryophyte layer dominated by *Sphagnum* spp. mosses but also including feather mosses (*Pleurozium* spp) and haircap mosses (*Polytrichum* spp). The peatland soil is the Greenwood series, a Typic Haplohemist (<http://www.websoilsurvey.nrcs.usda.gov>), with average peat depths to the Wisconsin glacial-age lake bed of 2–3 m, but depths up to 11 m are present (Parsekian et al., 2012). A further summary of the peat

geochemistry can be found in (Tfaily et al., 2014). Near-surface porewater pH is about 4.0 (Griffiths & Sebestyen, 2016).

The observational, pre-treatment data used in this study were compiled from a number of different research groups that collaborate as part of the SPRUCE project. One set of CH<sub>4</sub> flux observations was measured using a large-collar approach (Hanson et al., 2016, 2017). A second set of CH<sub>4</sub> flux observations was measured using an automatic chamber approach, and was used to validate the model performance (Gill et al., 2017). Meanwhile, surface water and porewater profiles of DOC concentrations were made by Griffiths and Sebestyen (2016); Zalman et al. (2018). The DOC concentration for surface and pore water were from Griffiths et al. (2017). The vertical concentration of CH<sub>4</sub> in the soil profile and soil DOC concentrations were measured are available at the SPRUCE experiment data portal (<https://mnspruce.ornl.gov/>). In addition to the CH<sub>4</sub>-related observations, we also used observations of vegetation growth and productivity to validate model simulations, ensuring the model produces reasonable estimates of vegetation inputs to the soil column. These observations include fine root production and standing crop (Iversen et al., 2017), allometric and biomass data on tree species (Hanson et al., 2012), and *Sphagnum* productivity (Norby & Childs, 2018). Model simulations calibrated using this vegetation information are presented in Griffiths et al. (2017) and Jensen et al. (2018).

## 2.2. Model Integration and Development

For this study, we implemented a new version of the Energy Exascale Earth System land model (ELM) designed for simulations at the SPRUCE site (hereafter referred to as ELM-SPRUCE). Our site-scale modeling framework explicitly predicts wetland hydrology, allowing for the application of a mechanistic framework that includes representation of the acetoclastic and hydrogenotrophic pathways for methanogenesis and tracks microbial populations in different functional groups. This framework also predicts how methanogenesis and methanotrophy are impacted by local water table and moisture variations. Other modeling groups have developed simulations frameworks with similar levels of mechanistic detail (e.g., Grant, 1998; Hopcroft et al., 2011; Martens et al., 1998; Xu & Tian, 2012), but this is the first application in the Community Land Model (CLM) and ELM frameworks to our knowledge. Our work improves upon CLM4Me (Riley et al., 2011), which is the pre-existing methane model available in ELM and the Community Land Model version 4.5 (CLM4.5), in which gridcell-averaged decomposition rates are used as a basis for computing CH<sub>4</sub> fluxes in inundated gridcell fractions. TECO-SPRUCE, which was also developed for the SPRUCE site, also includes a prognostic water table and CH<sub>4</sub> cycling (Ma et al., 2017), and has been used to assimilate and validate against observations. Both site-specific frameworks allow for a more comprehensive evaluation against available measurements, and the ability to predict potential changes in CH<sub>4</sub> production, consumption and transport related to temperature and CO<sub>2</sub> manipulation. However, our framework adds additional process complexity through its representation of explicit methanogenic pathways and microbial populations.

The new version of ELM-SPRUCE presented in this study integrates previously separate model developments for simulating wetland hydrology (Shi et al., 2015), methane cycling (Xu et al., 2015) and moss plant functional types (Shi et al., 2020; Walker et al., 2017). In addition to this model integration, we incorporate several new developments in this study for simulating wetland biogeochemistry that are described below. For the model integration, we began with the original version of ELM, which branched from the Community Land Model version 4.5 (CLM4.5) (Oleson et al., 2013). In ELM-SPRUCE, we added several improvements were made to meet the specific requirements for the hydrology in the ombrotrophic S1 Bog (Shi et al., 2015), including: revised hydrological parameters, the model representation of hummock and hollow microtopography, and lateral flows. A *Sphagnum* plant functional type incorporating the unique physiology of mosses module was also included (Shi et al., 2020; Walker et al., 2017). Finally, an improved CH<sub>4</sub> module first implemented by Xu et al. (2015) was integrated and further developed for this study. This study specifically focuses on the CH<sub>4</sub> module and its application at the SPRUCE site.

The newly integrated CH<sub>4</sub> module (Xu et al., 2015) replaces the existing CH<sub>4</sub> model in CLM4.5 (Riley et al., 2011) with a more mechanistic representation of biogeochemical processes related to CH<sub>4</sub> cycling. This new module represents CH<sub>4</sub> production and consumption in association with the existing decomposition subroutines in CLM4.5 (Thornton & Rosenbloom, 2005; Thornton et al., 2007). Added processes include DOC fermentation, methanogenesis based on H<sub>2</sub> and CO<sub>2</sub> (hydrogenotrophic methanogenesis),



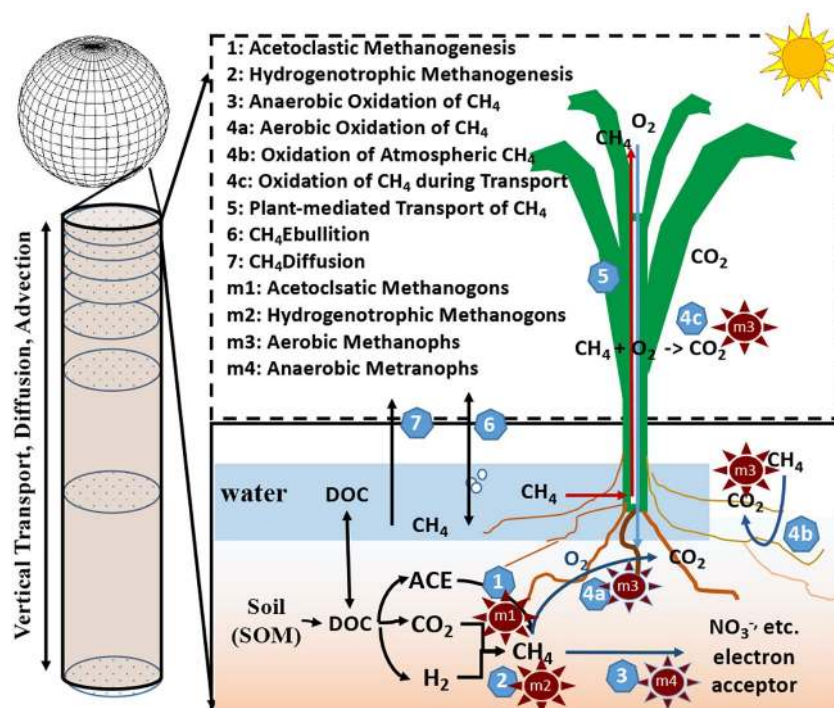


**Figure 1.** The primary improvements of soil biogeochemistry on the basis of Community Land Model version 4.5 (DOC, dissolved organic carbon; ACE, acetate; the numbers shown in the figure are corresponding to various processes; modified from Xu et al., 2015, 2016).

methanogenesis based on acetate (acetoclastic methanogenesis), aerobic methanotrophy, anaerobic methanotrophy, and  $H_2$  production (Figure 1). All of these mechanistic improvements were developed from known processes (Thauer et al., 1989, 2008), and/or adopted from approaches used in previous modeling studies (Grant, 1998, 1999; Kettunen, 2003; Riley et al., 2011; Segers & Kengen, 1998; Tian et al., 2010; Walter & Heimann, 2000; Zhuang et al., 2004). In addition, this model simulates a pH feedback because acetate formation increases the acidity of soils, which was also observed in incubation experiments (Xu et al., 2015). The detailed information for the  $CH_4$  module, including key parameters and model equations, can be referred in the Supporting Information S1. The simulated surface  $CH_4$  flux is the sum of diffusion, ebullition, and plant aerenchyma-mediated transport. Diffusion is a function of  $CH_4$  concentration and temperature in each layer, ebullition is a function of  $CH_4$  concentration and temperature in each layer; the plant aerenchyma mediated transport is a function of  $CH_4$  concentration, temperature, and root distribution in each layer and the temporal variation of net primary production. The  $CH_4$  concentration is the difference between methanogenesis and methanotrophy; both processes are simulated as a function of microbial biomass, microbial growth efficiency, temperature, soil pH, and oxygen availability (Xu et al., 2015; Wang et al., 2019).

Several further developments to the  $CH_4$  module were undertaken for this study. While Xu et al., (2015) performed CLM4.5 simulations using only one soil layer for the purposes of comparing against incubations, here we integrated the  $CH_4$  modeling into the full 10-layer soil decomposition model for the first time in ELM for the prediction of ecosystem-level responses. This involved adding three new pools for each soil layer: bacterial biomass, fungal biomass, and dissolved organic matter. Each pool has both carbon and nitrogen components. In addition to the 8 pre-existing litter and soil organic matter pools, ELM-SPRUCE now contains a total of 11 pools per soil layer with a total of 34 transitions between different pools and carbon respiration to the atmosphere and nitrogen cycling processes. The processes for carbon flow in and out of bacteria and fungi pools are adopted from (Xu et al., 2014). In addition to these pools, concentrations of dissolved organic carbon (DOC) and acetate are also tracked for each soil layer. Details are included in the Supporting Information S1.

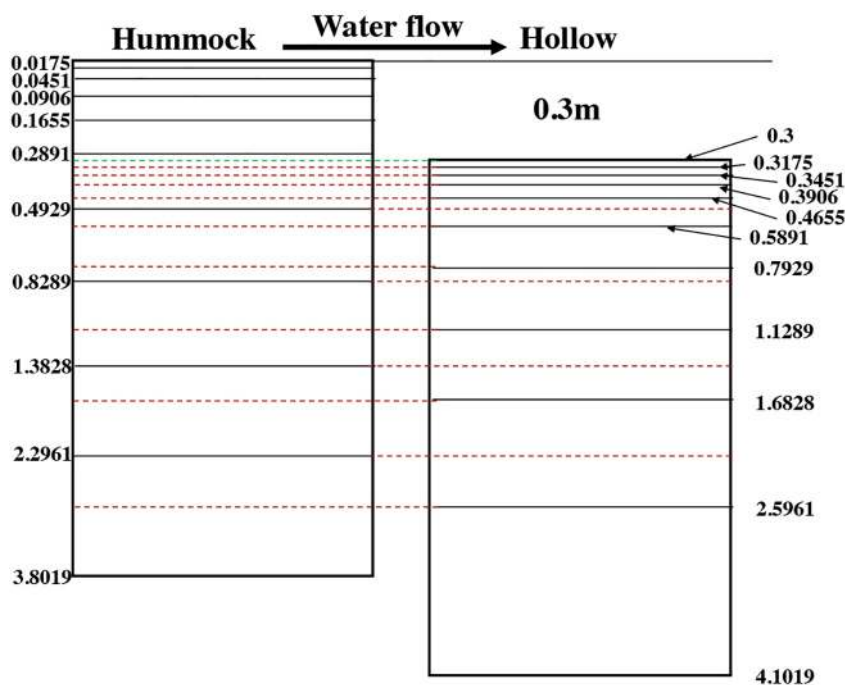


**Figure 2.** Vertical layer differentiation in hummock and hollow columns for simulating horizontal exchanges of biogeochemical variables (DOC, acetate, CO<sub>2</sub>, and CH<sub>4</sub> in this study). Each layer at the same height has horizontal exchange between the columns of biogeochemical variables along a concentration gradient. When multiple layers in one column correspond to one layer in the second column, contributions from each layer are averaged weighted by layer thickness at end of each time step.

We also extend the representation of lateral flows of water within the hummock-hollow microtopography in ELM-SPRUCE (Shi et al., 2015) to include flows of DOC, acetate, CO<sub>2</sub>, and CH<sub>4</sub>. To estimate biogeochemical processes contributing to CH<sub>4</sub> cycling, the consideration of both lateral and horizontal flows is critical (Cresto-Aleina et al., 2015; Kolka et al., 2011; Verry et al., 2011; Waddington et al., 2015). While Shi et al. (2015) only considered lateral and vertical flows of water in the soil column, we resolve biogeochemical transport and diffusion along these hydrological flow paths. Given our prescribed 30 cm vertical offset between the grid cells, we considered the vertical layers that corresponded to each other on an absolute elevation in the hummock and hollow grid cells. Lateral transport is only allowed between these corresponding layers. Because of the vertical offset between hummock and hollow grid cells, it is not a one-to-one mapping, so that in some cases multiple vertical layers in one grid cell may correspond to one layer in the other (Figure 2). The nutrient and gas concentrations in the new framework were aggregated to a standard vertical profile in ELM-SPRUCE for further calculation or simulation in other modules. The vertical diffusion of DOC, acetate, CO<sub>2</sub>, and CH<sub>4</sub> follows Fick's law along the concentration gradient.

The non-methane portions of the model (vegetation and hydrology) variables have been evaluated against observational data from multiple sources. In our previous ELM-SPRUCE study, we evaluated our modeled results for biogeophysical variables such as water table and evapotranspiration (Shi et al., 2015). ELM-SPRUCE simulated net ecosystem exchange is consistent within the uncertainty bounds of pre-treatment carbon budget estimates (Griffiths et al., 2017), and simulated vegetation productivity (Jensen et al., 2018).

### 2.3. Model Implementation

The model simulations are implemented in a workflow that includes several steps (Figure 3). In the first step, a spin-up simulation is used to generate pre-industrial steady-state values for carbon and nitrogen storage in vegetation and along the soil profile. This stage consists of accelerated decomposition (AD) spin-up and final spin-up following the standard approach of CLM4.5 (Oleson et al., 2013; Thornton & Rosenbloom, 2005). The accelerated spin-up generates an equilibrium state to estimate the relative

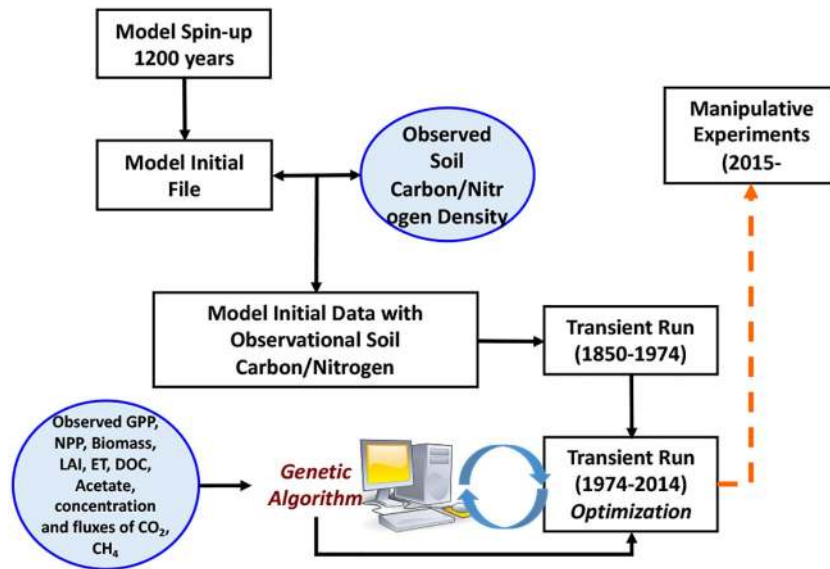


Figure 3. The procedure for model implementation.

content of carbon and nitrogen in different pools including four soil carbon pools and three litter carbon pools, as well as four soil nitrogen pool and three litter nitrogen pools, in each of 10 layers along the soil profile. The length of this AD spin-up is 1200 model years. After readjustment of carbon pools and turnover times following the AD spin-up, a final spin up of 50 years was carried out for re-equilibration. Because the model in its current form is not able to simulate the accumulation of peat, it produces a soil carbon that is, inconsistent with the observed profile. In the second step, after the model spin-up is finished, we re-initialize the soil carbon/nitrogen ratio by adjusting the simulated soil carbon and nitrogen profiles at each soil layer to best match field observations (Iversen et al., 2014; Tfaily et al., 2014). We then adjust the characteristic e-folding depth parameter (Koven et al., 2013) so that our adjustments to the soil carbon profile would not significantly affect the CO<sub>2</sub> emissions from each layer. This procedure allows for a soil carbon profile that is, consistent with observations while maintaining near steady-state fluxes (Table 1). Next, we perform a transient simulation from 1850-1974 in which atmospheric CO<sub>2</sub> concentrations and nitrogen deposition change over time. Finally, we simulate the period from 1974

to 2016, also using time-varying historical CO<sub>2</sub> concentrations and nitrogen deposition. The strip-cut that occurred in 1974 (Perala & Verry, 2011) is represented as a 99% harvest of above-ground tree biomass. In this phase, we also carry out a sensitivity analysis (Section 2.4) and parameter optimization (Section 2.5). After all the model calibration is completed, the optimized parameters are used for a complete set of new simulations from the beginning of spin up and transient runs, including the re-initialization of soil carbon after spin-up. For meteorological inputs for all phases of the simulation, we continuously cycle the observed SPRUCE environmental data (air temperature, wind speed, solar radiation, relative humidity, air pressure, and precipitation) from the period 2011–2017 that were obtained from an environmental monitoring station at the SPRUCE S1 bog (Hanson et al., 2015).

This identical model procedure was repeated for a second version of ELM-SPRUCE, in which the new CH<sub>4</sub> module was turned off and replaced with the default CLM4Me (Riley et al., 2011). This version still uses the Shi et al. (2015) hydrology and microtopography modifications in addition to modifications for the *Sphagnum* plant functional type.

**Table 1**  
The Initial Soil Carbon Pool Size for the Model Transient Simulation Starting in 1974

Soil depth (m)	Soil carbon density (gC m <sup>-3</sup> )	Soil carbon content (gC m <sup>-2</sup> )
0–0.018	22,385	392
0.018–0.045	22,385	617
0.045–0.091	22,385	1018
0.091–0.166	30,294	2271
0.166–0.289	43,978	5436
0.289–0.493	95,584	19,478
0.493–0.829	92,983	31,241
0.829–1.383	83,658	46,341
1.383–2.296	83,799	76,533
2.296–3.802	90,616	63,783



**Table 2**

*Ecological Meanings, Acceptable Ranges, and Optimized Values of the Key Parameters for CH<sub>4</sub> Processes Used in the Sensitivity Analysis and Optimization (Adopted From Xu et al., 2015)*

Parameters	Ecological meaning	Minimum	Maximum	Optimal
<i>m_dKAce</i>	Half saturation coefficient of available carbon mineralization	12.8	19.2	16.0
<i>m_dAceProdACmax</i>	Maximum rate for acetate production	$1.92 \times 10^{-6}$	$2.88 \times 10^{-6}$	$2.48 \times 10^{-6}$
<i>m_dH2ProdAcemax</i>	Maximum rate for H <sub>2</sub> production	$4.0 \times 10^{-8}$	$7.0 \times 10^{-8}$	$6.98 \times 10^{-8}$
<i>m_dGrowRH2Methanogens</i>	Hydrogenotrophic methanogen growth rate	$8.0 \times 10^{-3}$	$1.2 \times 10^{-2}$	$1.0 \times 10^{-2}$
<i>m_dDeadRH2Methanogens</i>	Hydrogenotrophic methanogen death rate	$8.0 \times 10^{-4}$	$1.2 \times 10^{-3}$	$1.0 \times 10^{-3}$
<i>m_dGrowRAceMethanogens</i>	Acetoclastic methanogen growth rate	$6.4 \times 10^{-3}$	$9.6 \times 10^{-3}$	$7.034 \times 10^{-3}$
<i>m_dDeadRAceMethanogens</i>	Acetoclastic methanogen death rate	$1.6 \times 10^{-3}$	$2.4 \times 10^{-3}$	$2.0 \times 10^{-3}$
<i>m_dGrowRMethanotrophs</i>	Methanotroph growth rate	$6.4 \times 10^{-3}$	$9.6 \times 10^{-3}$	$8.0 \times 10^{-3}$
<i>m_dDeadRMethanotrophs</i>	Methanotroph death rate	$1.6 \times 10^{-3}$	$2.4 \times 10^{-3}$	$2.0 \times 10^{-3}$
<i>M_dYAOMMethanotrophs</i>	Growth efficiency of anaerobic methanotrophs	0.12	0.18	0.15
<i>m_dACMinQ10</i>	Temperature dependence of acetate production	2.4	3.6	3.024
<i>m_dCH4ProdQ10</i>	Temperature dependence of CH <sub>4</sub> production	1.6	2.4	2.0
<i>m_dCH4OxidQ10</i>	Temperature dependence of CH <sub>4</sub> oxidation	0.96	1.44	1.20
<i>m_dCH4min</i>	Minimum CH <sub>4</sub> solubility	0.04	0.06	0.05
<i>k_dom</i>	Dissolved organic matter turnover rate	$5.6 \times 10^{-3}$	$8.4 \times 10^{-3}$	$7.004 \times 10^{-3}$
<i>k_bacteria</i>	Bacterial turnover rate	0.176	0.264	0.22
<i>k_fungi</i>	Fungal turnover rate	0.176	0.264	0.22
<i>dom_diffus</i>	Diffusion rate of dissolved organic matter	$1.44 \times 10^{-7}$	$2.16 \times 10^{-7}$	$1.8 \times 10^{-7}$
<i>m_dPlantTrans</i>	Efficiency for plant transport of CH <sub>4</sub>	$5.6 \times 10^{-3}$	$8.4 \times 10^{-3}$	$7.0 \times 10^{-3}$

#### 2.4. Sensitivity Analysis

Model sensitivity analysis is essential for model testing as it helps to apportion different sources of uncertainty in the model parameters or model structure (Cariboni et al., 2007; Haefner, 2005). Here we focus on model parameters, because understanding their sensitivities can provide mechanistic insight into which processes dominate the uncertainty of specific model outputs. A sensitivity analysis was carried out to estimate the model behavior in response to key parameters. In this sensitivity analysis, 19 selected model parameters controlling CH<sub>4</sub> processes were allowed to vary between −20% and +20% from their default values (Table 2). These parameters cover all key processes for CH<sub>4</sub> production, oxidation, and transport through plants, diffusion, and ebullition. We ran an ensemble of 2000 model simulations, randomly varying all parameters simultaneously over their prescribed ranges to identify both the most sensitive and the most stable parameters controlling the CH<sub>4</sub> processes. The computational expense of ELM-SPRUCES is high, requiring about 12 h per simulation on a single processor; therefore, we chose this sampling strategy to facilitate global sensitivity analysis using a surrogate model that is, constructed using Bayesian compressive sensing (Ricciuto et al., 2018; Sargsyan et al., 2014). This approach allowed for sensitivities with high confidence to be obtained with the 2000 model ensemble simulations, a relatively small number for this high-dimensional space. Simulations were performed both with ambient conditions, and +9°C, the highest level of warming the SPRUCES experiment following Griffiths et al. (2017) to understand how the treatments may affect the importance of different processes.

#### 2.5. Model Optimization Algorithm

An evolutionary algorithm, quantum particle swarm optimization (QPSO) (Sun et al., 2004), was used to optimize model parameters related to CH<sub>4</sub> cycling. Because some optimal parameter combinations were identified as unrealistic, we used a manual calibration approach for fine-tuning following the QPSO optimization. Allowable ranges for CH<sub>4</sub> parameters were the same as those used for the sensitivity analysis (Table 2).

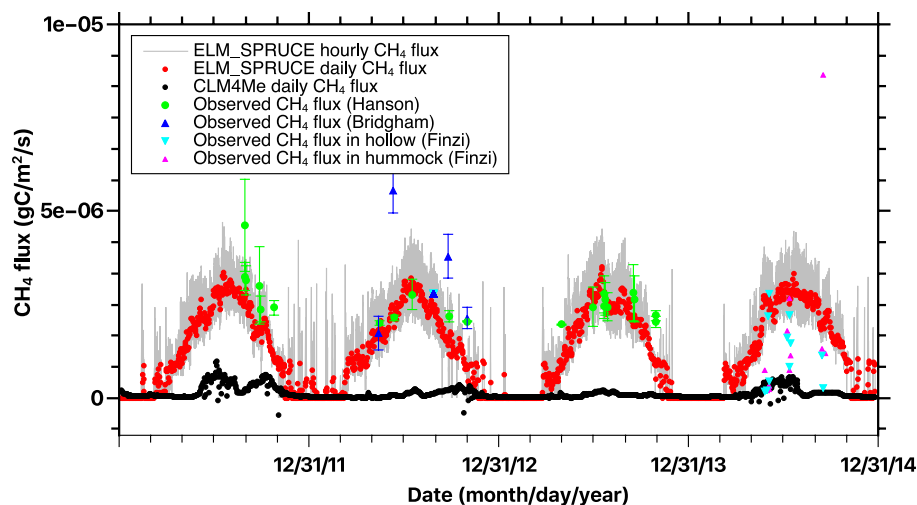


**Figure 4.** The comparison between modeled  $\text{CH}_4$  flux with measured  $\text{CH}_4$  from various sources fluxes measured in the field using different techniques.

The QPSO algorithm was used to minimize a cost function, which was constructed using a weighted sum of squared residuals (the difference between model and observation) for all  $\text{CH}_4$  related observations described in Section 2.1. Observational uncertainties, when available, were used for the weightings. When uncertainties were not available, we assumed the uncertainty to be 25% of the magnitude of the observed value. Here we used a population size of 50 and 100 iterations to perform the QPSO optimization. The final optimized parameters were the most consistent with the observational data in magnitude and seasonality. Additional fine tuning did not significantly affect the cost function value. More details about the QPSO algorithm and calibration approach are provided in Lu et al. (2017).

### 3. Results

#### 3.1. Model Validation

In this study, we specifically focus on  $\text{CH}_4$  cycling and compare modeled DOC,  $\text{CH}_4$  concentration and  $\text{CH}_4$  flux against observational data.

The ELM-SPRUCE model is able to capture the temporal variation in land surface  $\text{CH}_4$  flux at the S1 bog (Figure 4). The modeled daily  $\text{CH}_4$  fluxes display significant correlations with field observations and are well-aligned in terms of seasonality and magnitude ( $R^2 = 0.327$ ;  $P = 0.007$ ;  $\text{Mod} = 0.751 (0.248) \times \text{Obs} + 2.421\text{E-}8 (6.569\text{E-}7)$ ) for the large collars (Hanson et al., 2016). Predicting much lower flux magnitudes, the CLM4Me model has an insignificant correlation ( $R^2 = 0.112$ ,  $P = 0.137$ ;  $\text{Mod} = 0.062 (0.040) \times \text{Obs} + 1.488\text{E-}8 (1.056\text{E-}7)$ ). The ELM-SPRUCE model also compares well ( $R^2 = 0.581$ ;  $P = 0.078$ ;  $\text{Mod} = 0.089 (0.038) \times \text{Obs} + 1.427\text{E-}6 (3.337\text{E-}7)$ ) with the static chamber observations (Zalman et al., 2018), although the small number of measurements means that the results are less statistically significant. The large temporal variations in  $\text{CH}_4$  flux from the hummocks and hollows measured using the auto-chamber method (Gill et al., 2017) are less consistent with the daily modeled fluxes ( $R^2 < 0.05$ ). Additionally, while seasonally consistent in relative magnitude, the modeled fluxes were generally larger than the observed  $\text{CH}_4$  fluxes from hummocks and hollows; linear regression showed that the modeled fluxes overestimate the auto-chamber observations by about 10%. It is important to note that vegetation was removed in the auto-chambers, which was not considered in these simulations. There is also a timescale mismatch between the point-in-time observation (i.e., a timescale of minutes) and the daily model output. Therefore, the range of modeled hourly  $\text{CH}_4$  fluxes, which show higher variability, match better with these measured fluxes. The CLM4Me model did not have significant correlations with the static or autochamber flux data.

We also compared ELM-SPRUCE results to observed vertical profiles of substrates that are important for  $\text{CH}_4$  cycling. This further comparison showed that the model can reconstruct the vertical distributions of

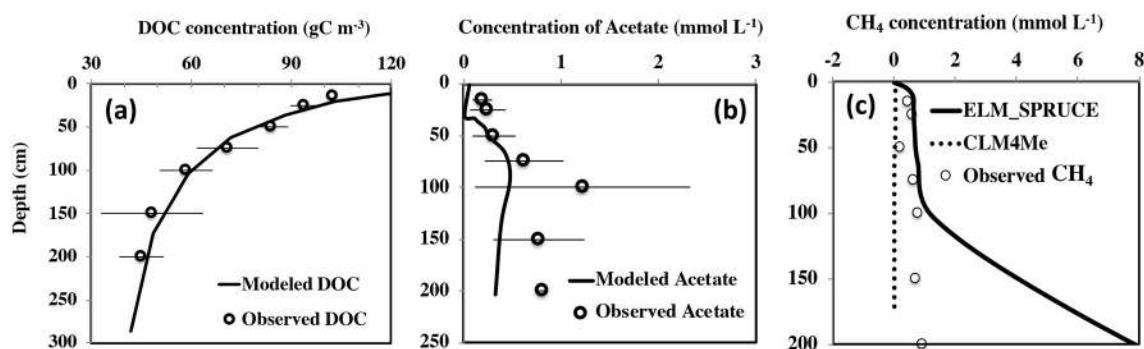


**Figure 5.** Model comparison with observational data of dissolved organic carbon (DOC), acetate, and CH<sub>4</sub> concentrations along soil profile (the concentration of DOC, acetate, and CH<sub>4</sub> are averages in the 2013 growing season).

DOC ( $R^2 = 0.974$ ;  $P < 0.001$ ;  $\text{Mod} = 0.958 (0.070) \times \text{Obs} + 6.672 (5.262)$ ) and acetate ( $R^2 = 0.588$ ;  $P = 0.044$ ;  $\text{Mod} = 0.448 (0.168) \times \text{Obs} + 0.042 (0.116)$ ). For CH<sub>4</sub> concentrations, the model reproduces the data well near the surface but not at depth ( $R^2 = 0.06$ ) (Figure 5). The gradually declining DOC concentration along the soil profile is well-captured by the model in both magnitude and distribution along the vertical profile, and the model is able to simulate the gradual decline in DOC concentration from  $\sim 100$  to  $30 \text{ g C m}^{-3}$  at 300 cm depth. The modeled vertical profile of acetate matched well with observed acetate concentration in the top 100 cm of the soil profile, while the modeled acetate concentration is slightly underestimated below 100 cm. The observed CH<sub>4</sub> concentration with depth in the upper meter of the soil profile was simulated, but performed poorly at deeper levels (Figure 5). The CLM4Me does not simulate DOC and acetate, while produces one order lower CH<sub>4</sub> concentration and inconsistent vertical CH<sub>4</sub> profile than the observed CH<sub>4</sub> concentration (Figure 5).

### 3.2. Sensitivity Analysis

A sensitivity analysis was carried out to estimate the CH<sub>4</sub> emissions and contributions to these emissions from three transport pathways under ambient conditions and under +9°C, the maximum level of warming in the SPRUCE experiment. While we varied 19 model parameters (described in Supporting Information S1), the surface CH<sub>4</sub> flux was sensitive to only five of these parameters—the maximum acetate production rate ( $m\_dAceProdACmax$ ), the methanogen growth rate ( $m\_dGrowRAceMethanogens$ ), the half-saturation coefficient of available carbon mineralization ( $m\_dKAce$ ), the dissolved organic matter turnover rate ( $k\_dom$ ), and the methanogen death rate ( $m\_dDeadRH2Methanogens$ ). The most sensitive parameter was the maximum production rate of acetate, indicating the importance of substrate regulation for CH<sub>4</sub> production. Under the +9°C warming condition, the contribution of acetate production rate weakened, while the mineralization rate of dissolved organic matter became more important. This shift suggests that while acetoclastic methanogenesis increases with warming, the warming may reduce the role of acetate as a substrate for methanogenesis but enhance the control from DOC, which might be caused by the faster decomposition rate of acetate compared to DOC.

For all three transport pathways, the half saturation coefficient of acetate is equally important. The sensitivities of other key parameters controlling the contribution to CH<sub>4</sub> surface flux from each of three transport pathways are different, providing important information for model parameterization (Figure 6). For example, the most sensitive parameter controlling CH<sub>4</sub> flux from plant-mediated transport under ambient conditions is the substrate production rate, followed by the growth rate of acetoclastic methanogens. Warming increased the sensitivity of the plant transport coefficient ( $m\_dPlantTrans$ ). CH<sub>4</sub> flux from the diffusion transport pathway is primarily controlled by the diffusion rate of dissolved organic matter ( $dom\_diffusion$ ), which is a key precursor for CH<sub>4</sub> production. The key parameters controlling CH<sub>4</sub> flux from ebullition are the maximum acetate production rate and the growth rate of acetoclastic methanogens. Warming increased the sensitivity of two parameters: the decomposition rate of DOC and plant transport. Shifts in importance among the three transport pathways also resulted in changes to parameter sensitivities for the integrated CH<sub>4</sub> flux at the surface. These sensitivities provide important information about the contributions of model

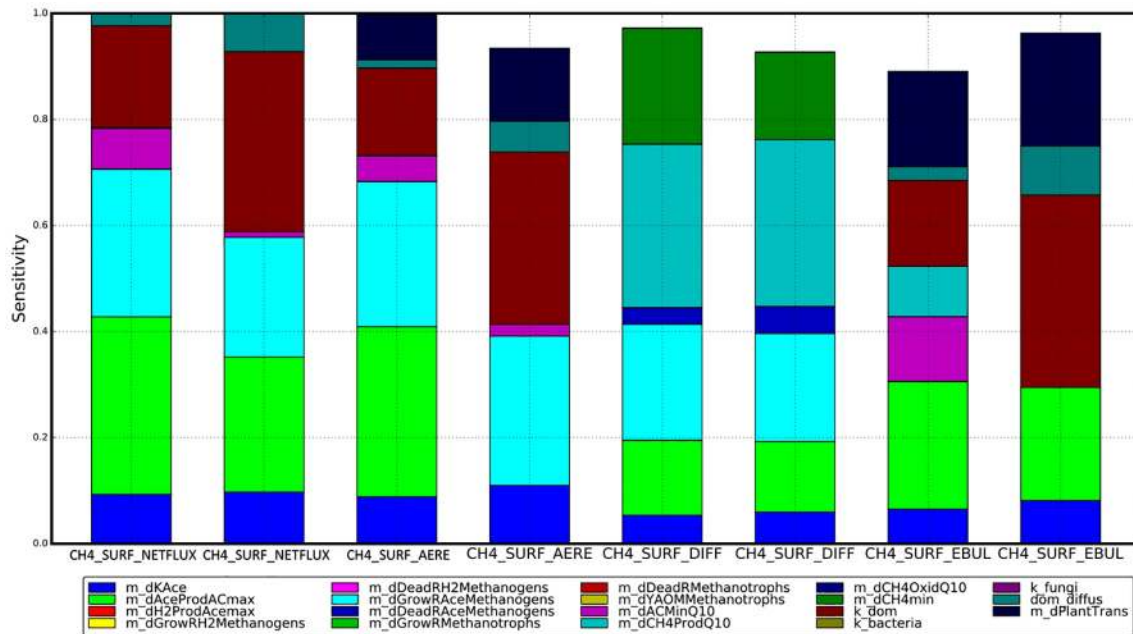


**Figure 6.** Sensitivity analysis of Energy Exascale Earth System land model-Spruce and Peatland Responses Under Changing Environments parameters for the following model outputs and scenarios: (a) Surface CH<sub>4</sub> flux under ambient conditions, (b) Surface CH<sub>4</sub> flux under the +9°C treatment, (c) Surface CH<sub>4</sub> flux from plant transport under ambient conditions, (d) Surface CH<sub>4</sub> flux from plant transport under the +9°C treatment, (e) Surface CH<sub>4</sub> flux from diffusion under ambient conditions, (f) Surface CH<sub>4</sub> flux from diffusion under the +9°C treatment, (g) Surface CH<sub>4</sub> flux from ebullition under ambient conditions, (h) Surface CH<sub>4</sub> flux from ebullition under the +9°C treatment. The height of each bar indicates the fraction of variance in a model output caused by variations in the corresponding model parameter. Stacked bars sum to one except in cases where higher-order parameter interactions are important (not shown).

processes to prediction uncertainty, and which quantities would be useful to better measure under ambient and warming conditions.

### 3.3. Modeled Surface CH<sub>4</sub> Flux Along the Three Transport Pathways

The modeled annual CH<sub>4</sub> net efflux from the S1 bog is estimated at 31 g C m<sup>-2</sup> y<sup>-1</sup>, close to the calculated annual CH<sub>4</sub> net efflux based on simple interpolation from time series of measured CH<sub>4</sub> flux (Hanson et al., 2016, 2017). The modeled CH<sub>4</sub> flux showed obvious seasonality in plant-mediated transport and ebullition, while the diffusion did not show a clear seasonal pattern (Figure 7). The model estimated that the ebullition, diffusion, and plant-mediated transport contributed approximately 61.5%, 15.0%, and 23.5%, respectively, to the CH<sub>4</sub> emissions to the atmosphere at an annual time scale (Figure 7). There is no modeled CH<sub>4</sub> emission in January, February, and March due to the frozen peat surface based on the assumption that the frozen surface prevents all CH<sub>4</sub> emissions from soil. Because of the buildup of CH<sub>4</sub> beneath these frozen layers, the model simulates an early spring CH<sub>4</sub> pulse when the frozen soil thaws in the spring.

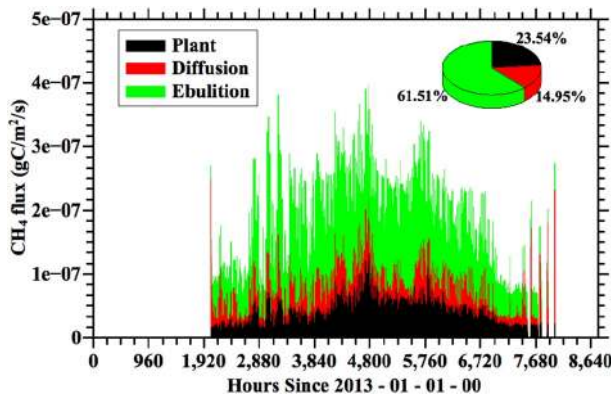


**Figure 7.** The modeled CH<sub>4</sub> transport pathways and their contributions to the annual budget of CH<sub>4</sub> emission from the S1 bog under ambient condition (hourly step is adopted to better demonstrate the CH<sub>4</sub> dynamic at a high temporal resolution). The pie chart shows the total contribution for each pathway to the annual sum of CH<sub>4</sub> emissions.

### 3.4. Differences Caused by Microtopography

Hummock and hollows are unique microtopographical features in peatland ecosystems. ELM-SPRUCE assumes a 0.3 m elevational difference between two adjacent grids to represent a “mean hummock” and a “mean hollow.” The simulated surface CH<sub>4</sub> flux and water table dynamics are



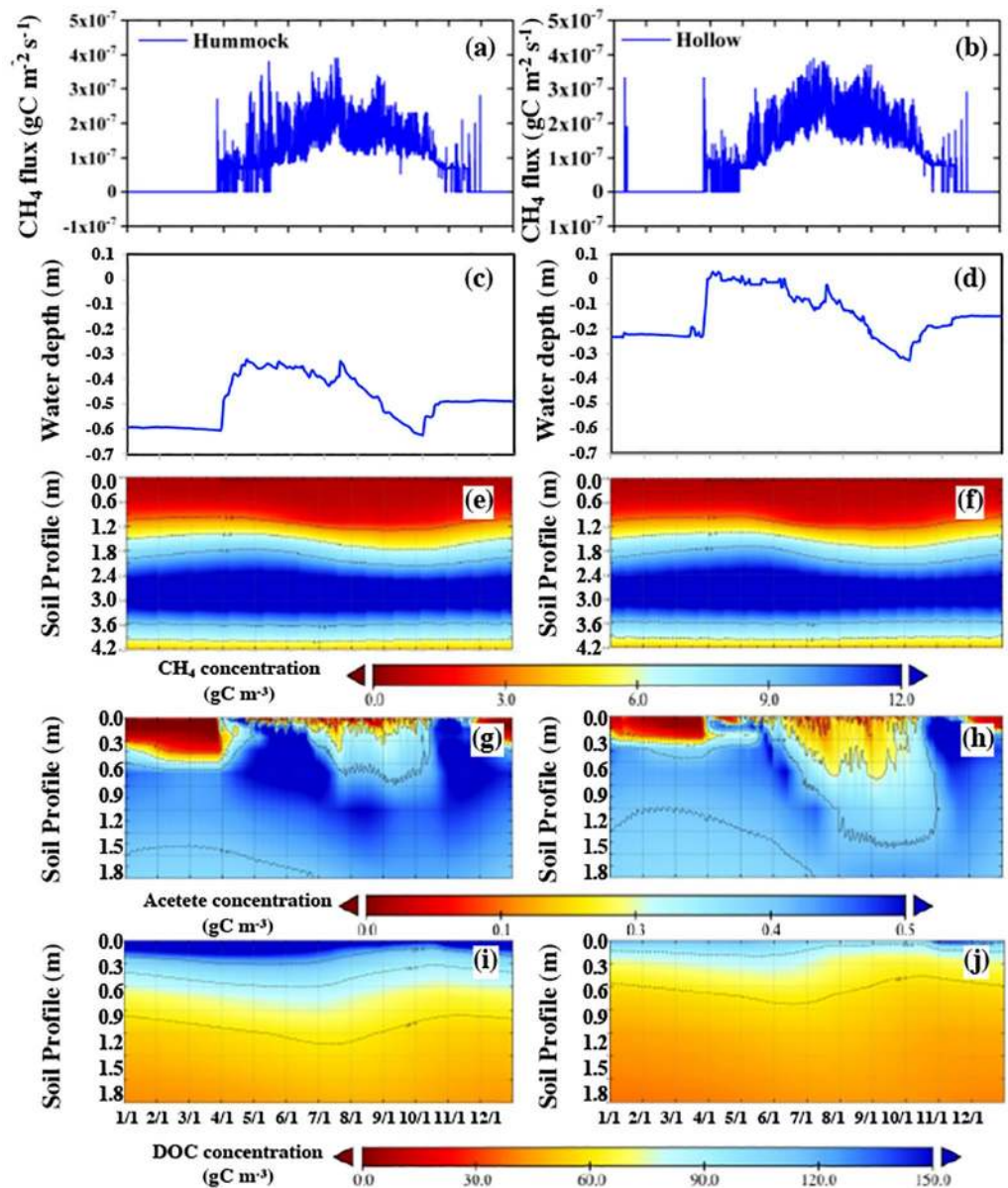


**Figure 8.** Seasonality in the vertical profiles of dissolved organic carbon (DOC), acetate, and  $\text{CH}_4$  concentration and their resultant surface  $\text{CH}_4$  flux and surface water table dynamics for hummock and hollow columns in 2013 (a) Surface  $\text{CH}_4$  flux from hummocks; (b) Surface  $\text{CH}_4$  flux from hollows; (c) Water table dynamics in hummocks; (d) Water table dynamics in hollows; (e) Soil/water profile of  $\text{CH}_4$  concentration in hummocks; (f) Soil/water profile of  $\text{CH}_4$  concentration in hollows; (g) Soil/water profile of acetate concentration in hummocks; (h) Soil/water profile of acetate concentration in hollows; (i) Soil/water profile of DOC concentration in hummocks; (j) Soil/water profile of DOC concentration in hollows; notice the difference in the Y-axis scale for water table between panels (c) and (d).

only slightly different, while the belowground hydrology and biogeochemistry are different for hummock and hollow (Figure 8).

The vertical offset between the two columns and lateral transport between them cause a lower position of the water table in hummocks compared to hollows generally equal to the specified difference in height between them (0.3 m). There are slight differences in annual  $\text{CH}_4$  flux between hummocks and hollows with consistent seasonal patterns between the two columns. A  $\text{CH}_4$  pulse in the early growing season was simulated for both hummocks and hollows, with a slightly stronger pulse in hollows than hummocks. Temporal patterns of water table variations are similar for the two columns when there is no standing water in



hollows ( $WT < 0$  for Hollow). When there is standing water in the hollow, there are substantial variations between the two columns due to horizontal flows and surface runoff from the hollows. Similar vertical patterns of DOC, acetate, and  $CH_4$  concentrations occur for hummocks and hollows, with slightly higher concentrations in hummocks than in hollows. Meanwhile, there are apparent differences in  $CH_4$ , acetate and DOC concentration at the soil depth of  $\sim 0.3$  m in hummocks versus hollows, which is consistent with the assumption of 0.3 m elevation difference in the surface of hummocks and hollows.

## 4. Discussion

### 4.1. Controls on $CH_4$ Flux and Transport Pathways

The ranking of all parameters responsible for  $CH_4$  flux and transport using a sensitivity analysis can be used to indicate the most essential processes contributing to surface  $CH_4$  fluxes and the most critical field measurements needed to better understand and predict  $CH_4$  fluxes in response to environmental change. Simulated warming does change the relative importance of the parameters controlling  $CH_4$  processes, indicating the critical impacts of warming on biogeochemical processes. Specifically with warming, the turnover rate of dissolved organic matter ( $k_{dom}$ ) becomes a more sensitive parameter, indicating the need for observations of this quantity under the experimental treatments. The sensitivity of this parameter in addition to other parameters associated with acetoclastic methanogenesis indicate the importance of this process under environmental change.

The sensitivity analysis showed that the most important process for  $CH_4$  dynamics in our model is acetoclastic methanogenesis, followed by the rate of acetate production, indicating that environmental factors controlling acetoclastic methanogenesis are likely the most important parameter(s) for the land-atmosphere  $CH_4$  flux (Xu et al., 2015). For example, acetate porewater concentration, water content in the field controlling acetate production, and plant root exudation have been confirmed to be critical in affecting  $CH_4$  flux (Conrad, 1989; Whiting & Chanton, 1993; Zona et al., 2009). The impacts of warming on the simulated fluxes will be discussed further in a subsequent manuscript.

The sensitivity analysis confirmed the importance of substrate production and microbial functional groups as two important determinants on  $CH_4$  cycling, indicating substrate limitation in the peatland and microbial suppression. This is consistent with previous field studies for substrate limitation of  $CH_4$  production (Hatala et al., 2012; McEwing et al., 2015). The substrate for  $CH_4$  production may come from soil organic matter mineralization or vegetation root exudation. Further experiment and modeling traceability are needed to address this issue. Carbon dioxide and  $CH_4$  isotopic capability in this model might be a useful solution to this issue, and it deserves future efforts.

The optimized version of the model generally produced accurate predictions of  $CH_4$  fluxes. This result is consistent with the results of a previous SPRUCE modeling study (Ma et al., 2017). That study involved parameter optimization and sensitivity analysis using the TECO-SPRUCE model, which has reduced complexity of  $CH_4$  and vegetation modules compared to ELM-SPRUCE. That study found a stronger influence of temperature sensitivity parameters on surface  $CH_4$  fluxes, suggesting that model may be more responsive to experimental warming. Ma et al. (2017) also predicted a higher contribution of plant-mediated transport to  $CH_4$  fluxes, suggesting that changes in vegetation composition may be more important in their model for predicting responses to warming treatments. These sensitivity analyses indicated that differences in model structure are likely contributing to a divergence in predictions despite calibration using pre-treatment observations. A companion paper to this study using ELM-SPRUCE to conduct warming simulations indeed indicates a muted warming response of  $CH_4$  fluxes compared to the TECO study (Yuan et al., 2021). This highlights the need for additional studies at the site using multiple models. As a result, we have initiated a model intercomparison project for this purpose.

One specific concern for the ELM-SPRUCE predictions is the overestimation of modeled  $CH_4$  flux compared with auto-chamber measurements of  $CH_4$  flux in hummocks and hollows despite closer agreement with the other two measurement methods. This may be due in part to the experimental design. Specifically, in the auto-chamber experiments, aboveground vascular vegetation was clipped limiting plant-mediated transport and root exudation of labile DOM (Gill et al., 2017). Before clipping, the auto-chambers gave similar  $CH_4$  fluxes to those measured by (Hanson et al., 2016). The reported  $CH_4$  flux from auto-chamber

method is ~10%–30% lower than the flux obtained with large-collar approach and static chamber approach that capture a portion of the vegetation (Figure 4). In the future, model simulations could be designed to replicate this effect by performing simulations without the presence of specific vegetation types. Our study estimated that ebullition accounts for 23.5% of the CH<sub>4</sub> flux, which is much larger than the 1% estimated by Gill et al. (2017). The reason might be that small area (0.3 m diameter of the collar) in that study excluded open water, where ebullition usually occurs, and their approach only captures larger bubbles that were identified by non-linearities in CH<sub>4</sub> emissions. Other studies show that smaller bubbles may be an important source of ebullition (Prairie & del Giorgio, 2013). Overall our estimate falls in the range of 10–60% as reported by a large number of field experiments (Chanton et al., 1989; Mer & Roger, 2001; Tokida et al., 2007).

#### 4.2. Key Features of the New Model

There are several key features of this new version of ELM-SPRUCE. First, the model integrates improvements in soil biogeochemistry and CH<sub>4</sub> dynamics described here with previous hydrologic improvements for two microtopography columns and parallel efforts to include a representation of moss. While previous modeling efforts have generally focused on specific components of wetland systems, these improvements allow for simulations with mechanistic representation of vegetation, hydrology, and soil biogeochemistry processes simultaneously, and this in turn can facilitate the examination of key feedbacks at the SPRUCE site. The vertically resolved representation of the model structure is critical for ecosystems with complex, depth-dependent belowground mechanisms, such as peatlands. In addition, the representation of site-specific plant functional types will allow exploration of how differences in productivity and mortality among these types may impact the site soil biogeochemistry under environmental change. For example, the recently observed decline in *Sphagnum* productivity (Norby et al., 2019) and shifts in the vascular plant community composition may have profound impacts on CH<sub>4</sub> cycling.

The highly mechanistic representation of biogeochemistry also allows model integration with the multiple types of observational data that are being collected as part of the SPRUCE experiment. For example, in this study, we compared the model output with observational data for CH<sub>4</sub> substrates, CH<sub>4</sub> concentration, and different transport pathways, in addition to the surface flux. This modeling approach provides a framework to understand how CH<sub>4</sub> dynamics respond to external environmental change. Meanwhile, this model is able to test the similar stimulation impacts of warming and elevated CO<sub>2</sub> on CH<sub>4</sub> flux with different mechanisms, which will be explored in future work. As the treatment data streams become available, we expect to simultaneously integrate this information with ELM-SPRUCE, continuously improving model performance and developing a mechanistic understanding of key processes and feedbacks contributing to carbon cycle responses. The model will also help to identify key processes, pools and temperature responses that experimentalists need to measure further to constrain key prediction uncertainties.

Importantly, ELM-SPRUCE allows us to determine if it is necessary to include this level of biogeochemical detail to successfully model the effects of warming and elevated CO<sub>2</sub> on CH<sub>4</sub> dynamics. The simpler TECO modeling framework has been a useful and highly successful testbed for an integrative approach, having been used to assimilate data on soil processes and snow (Huang et al., 2017), vegetation and soil carbon cycling (Jiang et al., 2018) and methane (Ma et al., 2017) in an ecological forecasting framework (Huang et al., 2019). ELM-SPRUCE, a considerably more complex and computationally demanding model, is currently being integrated into this forecasting framework using novel, efficient techniques for model-data integration (Lu et al., 2018). ELM-SPRUCE will allow additional valuable sources of data to be integrated into the model that are already being collected in the experimental enclosures, including vegetation productivity for specific functional types, DOM and acetate concentration profiles, CH<sub>4</sub> production profiles, measurements of microbial biomass, and partitioning of acetoclastic and hydrogenotrophic methanogenesis through isotopic analysis.

#### 4.3. Importance of Model Timestep

The timestep of model output also affects the model performance in comparison with field observational data. This study showed that the hourly output is more consistent with observational CH<sub>4</sub> flux than the modeled daily CH<sub>4</sub> flux. We infer that the observational data tend to be highly variable with finer time steps,

which is consistent with the upscaling of ecosystem function. For example, the range of hourly flux in CH<sub>4</sub> is much wider than the daily flux (Figure 4). This is primarily caused by the large variation of temperature and precipitation at a sub-daily level. It is well known that the finer-scale ecosystem functions are more variable compared with coarse scale results (Hatala et al., 2012), and aggregating over space or time, if possible, may be necessary for comparison with models. It is important to conduct model evaluation at appropriate time scales to match the observational data, but also experimental designs should consider the appropriate time scale on which the ecosystem functions are measured and evaluated to maximize their relevance for modeling frameworks.

## 5. Conclusions and Future Directions

Here we extend the ELM-SPRUCE model (Griffiths et al., 2017; Shi et al., 2015) to include new capabilities for predicting CH<sub>4</sub> fluxes and variables associated with underlying production, oxidation, and transport mechanisms. ELM-SPRUCE is now an integrative site-scale model that simulates CH<sub>4</sub> dynamics from multiple perspectives including CH<sub>4</sub> substrate, CH<sub>4</sub> concentration in the soil profile, surface flux of CH<sub>4</sub>, transport pathways, and microbial mechanisms driving the production and oxidation of CH<sub>4</sub>. The model is used to predict pre-treatment conditions at the SPRUCE experiment site in a northern Minnesota peatland ecosystem. When model parameters are optimized using observations, the model accurately predicts the magnitude of and seasonal variations in CH<sub>4</sub> fluxes, as well as vertical profiles of DOC, acetate, and CH<sub>4</sub> within the peat layers. A parameter sensitivity analysis indicates that several parameters dominate uncertainties in CH<sub>4</sub> flux predictions including the turnover rate of dissolved organic matter, the maximum acetate production rate, and the growth rate of acetoclastic methanogens. Temperature sensitivity parameters are less important than indicated by previous studies. Our modeling framework, implemented within an Earth system model, lends itself naturally to regional and global scaling.

In the future, we expect improvements from ELM-SPRUCE to be fully integrated into the land component of the E3SM climate model. However, there are significant limitations in the current model structure and methods for spatial scaling that must be addressed to extend our model for regional and global relevance. Extending the ELM-SPRUCE model to account for variations in hydrology, vegetation, and sources of CH<sub>4</sub> fluxes over space and time is critical for eventual inclusion in an Earth system model. Variations in hydrology may strongly affect vegetation growth and peat decomposition with feedbacks on microtopography and peat properties, leading to different site microclimates and substrates for CH<sub>4</sub> processes (Waddington et al., 2015). Understanding how microtopography, hydrologic state variables and CH<sub>4</sub> fluxes are related is critical. Small differences in microtopography and developmental state can cause large differences in CH<sub>4</sub> emissions at seemingly similar sites, emphasizing the need for mechanistically based scaling techniques (Zalman et al., 2018). Microtopographic characteristics are currently observed with high accuracy at regular time intervals within the enclosures using terrestrial laser scanning (Graham et al., 2020), and this work could be extended over larger spatial scales, providing a key input for model-based scaling and parameterization of the Shi et al. (2015) hydrology module in ELM-SPRUCE over larger spatial scales. A spatially explicit version of ELM-SPRUCE must also have the ability to predict changes in vegetation productivity and community composition from warming and eCO<sub>2</sub> that likely feed back to CH<sub>4</sub> cycling. Ecosystem warming has already caused substantial changes to vegetation phenology at the SPRUCE site (Richardson et al., 2018), and changes in vegetation community composition may affect the ecosystem structure and function (Johnson et al., 2005), leading to different responses of CO<sub>2</sub> and CH<sub>4</sub> fluxes over long timescales (Ward et al., 2013). The introduction of dynamic vegetation into ELM-SPRUCE, for example, by integrating the Ecosystem Demography and CLM4.5 models (Fisher et al., 2015) is necessary to predict a realistic temporal evolution of vegetation across a range of sites. Finally, including isotopic tracers in our simulations is also necessary to trace the sources of the surface CH<sub>4</sub> flux and compare to observations across different sites. For example, homoacetogenesis is a key process for methanogenesis (Ye et al., 2014). At SPRUCE, it has been shown that this homoacetogenesis is an important process, that rates increase with temperature, and is important in the competition for H<sub>2</sub> with hydrogenotrophic methanogenesis (Leeways, 2019). An isotopic module will enhance our understanding of this process and its influence on surface CH<sub>4</sub> fluxes. <sup>13</sup>C and <sup>14</sup>C have already been incorporated in the current ELM version, but the isotopic module needs to be extended to

represent the effects CH<sub>4</sub> production and oxidation and other microbial processes (e.g., homoacetogenesis) on these isotopes.

A key goal of our ELM-SPRUCE modeling effort is eventual application to other wetland systems. A promising result for eventual spatial upscaling is that carbon cycle model simulations at wetland eddy covariance sites are fairly accurate in predicting gross and net carbon fluxes, especially when the models include realistic hydrology (Sulman et al., 2012). A mechanistic model-based upscaling will help integrate the observations obtained with site-level enclosure measurements with CO<sub>2</sub> and CH<sub>4</sub> fluxes measured to the larger footprints of eddy covariance towers over wetland sites. We can then assess the accuracy of these simulations across a variety of wetland tower sites, and better understand how key model sensitivities vary across sites using established methods (Ricciuto et al., 2018). Global simulations may then be performed using existing CH<sub>4</sub> modeling protocols (e.g., Melton et al., 2013). This will allow us to better understand the implications of the ambitious SPRUCE experiment for global peatlands, carbon cycling and terrestrial feedbacks to the climate system.

### Data Availability Statement

Model code used in these simulations are available on the Github repository at <http://doi.org/10.5281/zenodo.3733924>. Model simulation output used in this analysis will be made publicly available on the SPRUCE project website <https://mnspruce.ornl.gov> and can be accessed at <https://doi.org/10.25581/spruce.082/1638024>.

### Acknowledgments

This material is based upon work supported by the US Department of Energy, Office of Science, Office of Biological and Environmental Research. Oak Ridge National Laboratory is managed by UT-Battelle, LLC, for the US Department of Energy under contract DE-AC05-00OR22725. The views expressed in this article do not necessarily represent the views of the US Department of Energy or the United States Government. The authors would like to thank Randall K. Kolka, USDA Forest Service, Northern Research Station for working in collaboration with the Oak Ridge National Laboratory to enable access to and use of the S1-Bog of the Marcell Experimental Forest for the SPRUCE experiment and affiliated studies. This research used resources of the Compute and Data Environment for Science (CADES) at the Oak Ridge National Laboratory, which is supported by the Office of Science of the U.S. Department of Energy under Contract No. DE-AC05-00OR22725.

### References

- Blodau, C. (2002). Carbon cycling in peatlands—A review of processes and controls. *Environmental Reviews*, 10(2), 111–134. <https://doi.org/10.1139/a02-004>
- Bohn, T. J., Melton, J. R., Akihiko, I., Kleinen, T., Spahni, R., Stocker, B., et al. (2015). WETCHIMP-WSL: Intercomparison of wetland methane emissions models over West Siberia. *Biogeosciences*, 12, 3321–3349. <https://doi.org/10.5194/bg-12-3321-2015>
- Bridgman, S. D., Cadillo-Quiroz, H., Keller, J. K., & Zhuang, Q. (2013). Methane emissions from wetlands: Biogeochemical, microbial, and modeling perspective from local to global scales. *Global Change Biology*, 19(5), 1325–1346. <https://doi.org/10.1111/gcb.12131>
- Cariboni, J., Gatelli, D., Liska, R., & Saltelli, A. (2007). The role of sensitivity analysis in ecological modelling. *Ecological Modelling*, 203, 167–182. <https://doi.org/10.1016/j.ecolmodel.2005.10.045>
- Chanton, J. P., Martens, C. S., & Kelley, C. A. (1989). Gas transport from methane-saturated, tidal freshwater and wetland sediments. *Limnology & Oceanography*, 34(5), 807–819. <https://doi.org/10.4319/lo.1989.34.5.0807>
- Conrad, R. (1989). Control of methane production in terrestrial ecosystems. In M. O. Andreae, & D. S. Schimel (Eds.), *Exchange of trace gases between terrestrial ecosystems and the atmosphere* (pp. 39–58). Springer.
- Cresto-Aleina, F., Runkle, B. R. K., Kleinen, T., Kutzbach, L., Schneider, J., & Brovkin, V. (2015). Modeling micro-topographic controls on boreal peatland hydrology and methane fluxes. *Biogeosciences Discussions*, 12, 10195–10232. <https://doi.org/10.5194/bg-12-5689-2015>
- Fisher, R., Muszala, S., Versteinstein, M., Lawrence, P., Xu, C., McDowell, N., et al. (2015). Taking off the training wheels: The properties of a dynamic vegetation model without climate envelopes, CLM4. 5. *Geoscientific Model Development*, 8(11), 3593–3619. <https://doi.org/10.5194/gmd-8-3593-2015>
- Frolking, S., Talbot, J., Jones, M., Treat, C. C., Kauffman, J. B., Tuittila, E. S., & Roulet, N. T. (2011). Peatlands in the Earth's 21st century climate system. *Environmental Reviews*, 19, 371–396. <https://doi.org/10.1139/a11-014>
- Gill, A. L., Giasson, M. A., Yu, R., & Finzi, A. C. (2017). Deep peat warming increases surface methane and carbon dioxide emissions in a black spruce dominated ombrotrophic bog. *Global Change Biology*, 23(12), 5398–5411.
- Graham, J. D., Glenn, N. F., Spaete, L. P., & Hanson, P. J. (2020). Characterizing Peatland Microtopography Using Gradient and Microform-Based Approaches. *Ecosystems*, 23, 1464–1480.
- Grant, R. (1999). Simulation of methanotrophy in the mathematical model ecosys. *Soil Biology and Biochemistry*, 31(2), 287–297. [https://doi.org/10.1016/S0038-0717\(98\)00119-9](https://doi.org/10.1016/S0038-0717(98)00119-9)
- Grant, R. F. (1998). Simulation of methanogenesis in the mathematical model ecosys. *Soil Biology and Biochemistry*, 30, 883–896. [https://doi.org/10.1016/S0038-0717\(97\)00218-6](https://doi.org/10.1016/S0038-0717(97)00218-6)
- Griffiths, N. A., Hanson, P. J., Ricciuto, D. M., Iversen, C. M., Jensen, A. M., Malhotra, A., et al. (2017). Temporal and spatial variation in peatland carbon cycling and implications for interpreting responses of an ecosystem-scale warming experiment. *Soil Science Society of America Journal*, 81(6), 1668–1688. <https://doi.org/10.2136/sssaj2016.12.0422>
- Griffiths, N. A., & Sebestyen, S. D. (2016). Dynamic vertical profiles of peat porewater chemistry in a northern peatland. *Wetlands*, 36(6), 1119–1130. <https://doi.org/10.1007/s13157-016-0829-5>
- Haefner, J. W. (2005). *Modeling biological systems-principles and applications*. Springer.
- Hanson, P., Brice, D., Garten, C., Hook, L., Phillips, J., & Todd, D. (2012). *SPRUCE S1 bog vegetation allometric and biomass data: 2010–2011*. Oak Ridge National Lab's Terrestrial Ecosystem Science Scientific Focus Area.
- Hanson, P. J., Gill, A. L., Xu, X., Phillips, J. R., Weston, D. J., Kolka, R. K., et al. (2016). Intermediate-scale community-level flux of CO<sub>2</sub> and CH<sub>4</sub> in a Minnesota peatland: Putting the SPRUCE project in a global context. *Biogeochemistry*, 129(3), 255–272. <https://doi.org/10.1007/s10533-016-0230-8>
- Hanson, P. J., Riggs, J. S., Nettles, W. R., Phillips, J. R., Krassovski, M. B., Hook, L. A., et al. (2017). Attaining whole-ecosystem warming using air and deep-soil heating methods with an elevated CO<sub>2</sub> atmosphere. *Biogeosciences*, 14, 861–883. <https://doi.org/10.5194/bg-14-861-2017>



- Hanson, P., Riggs, J., Nettles, W., Krassovski, M., & Hook, L. (2015). *SPRUCe deep peat heating (DPH) environmental data, February 2014 through July 2015*. Oak Ridge National Lab's Terrestrial Ecosystem Science Scientific Focus Area.
- Hatala, J. A., Detto, M., & Baldocchi, D. D. (2012). Gross ecosystem photosynthesis causes a diurnal pattern in methane emission from rice. *Geophysical Research Letters*, 39(6), L06409. <https://doi.org/10.1029/2012gl0151303>
- Hopcroft, P. O., Valdes, P. J., & Beerling, D. J. (2011). Simulating idealized Dansgaard-Oeschger events and their potential impacts on the global methane cycle. *Quaternary Science Reviews*, 30, 3258–3268. <https://doi.org/10.1016/j.quascirev.2011.08.012>
- Huang, Y., Jiang, J., Ma, S., Ricciuto, D., Hanson, P. J., & Luo, Y. (2017). Soil thermal dynamics, snow cover, and frozen depth under five temperature treatments in an ombrotrophic bog: Constrained forecast with data assimilation. *Journal of Geophysical Research: Biogeosciences*, 122(8), 2046–2063. <https://doi.org/10.1002/2016jg003725>
- Huang, Y., Stacy, M., Jiang, J., Sundi, N., Ma, S., Saruta, V., et al. (2019). Realized ecological forecast through an interactive ecological platform for assimilating data (EcoPAD, v1. 0) into models. *Geoscientific Model Development*, 12(3), 1119–1137. <https://doi.org/10.5194/gmd-12-1119-2019>
- Iversen, C., Hanson, P., Brice, D., Phillips, J., McFarlane, K., Hobbie, E., & Kolka, R. (2014). *SPRUCe peat physical and chemical characteristics from experimental plot cores, 2012*. Oak Ridge National Lab's Terrestrial Ecosystem Science Scientific Focus Area.
- Iversen, C. M., McCormack, M. L., Powell, A. S., Blackwood, C. B., Freschet, G. T., Kattge, J., et al. (2017). A global fine-root ecology database to address below-ground challenges in plant ecology. *New Phytologist*, 215(1), 15–26. <https://doi.org/10.1111/nph.14486>
- Jensen, A., Warren, J., Hook, L., Wullschlegel, S., Brice, D., Childs, J., & Vander Stel, H. (2018). *SPRUCe S1 bog pretreatment seasonal photosynthesis and respiration of trees, shrubs, and herbaceous plants, 2010–2015*. Oak Ridge National Lab's Terrestrial Ecosystem Science Scientific Focus Area.
- Jiang, J., Huang, Y., Ma, S., Stacy, M., Shi, Z., Ricciuto, D. M., et al. (2018). Forecasting responses of a northern peatland carbon cycle to elevated CO<sub>2</sub> and a gradient of experimental warming. *Journal of Geophysical Research: Biogeosciences*, 123(3), 1057–1071. <https://doi.org/10.1002/2017jg004040>
- Johnson, W. C., Millett, B., V., Gilmanov, T., Voldseth, R. A., Guntenspergen, G. R., & Naugle, D. E. (2005). Vulnerability of northern prairie wetlands to climate change. *BioScience*, 55(10), 863–872. [https://doi.org/10.1641/0006-3568\(2005\)055\[0863:vonpw\]2.0.co;2](https://doi.org/10.1641/0006-3568(2005)055[0863:vonpw]2.0.co;2)
- Kettunen, A. (2003). Connecting methane fluxes to vegetation cover and water table fluctuations at microsite level: A modeling study. *Global Biogeochemical Cycles*, 17(2). <https://doi.org/10.1029/2002GB001958>
- Kolka, R. K., Sebestyen, S. D., Verry, E. S., & Brooks, K. N. (2011). *Peatland biogeochemistry and watershed hydrology at the Marcell Experimental Forest*. CRC Press.
- Koven, C. D., Riley, W., Subin, Z. M., Tang, J., Torn, M. S., Collins, W. D., et al. (2013). The effect of vertically-resolved soil biogeochemistry and alternate soil C and N models on C dynamics of CLM4. *Biogeosciences*, 10, 7109–7131. <https://doi.org/10.5194/bg-10-7109-2013>
- Leeways, C. (2019). *Soil warming effects on methane production pathways and homoacetogenesis in a northern Minnesota peatland (Master's thesis)*. Department of Biology, University of Oregon.
- Lu, D., Ricciuto, D., Stoyanov, M., & Gu, L. (2018). Calibration of the E3SM land model using surrogate-based global optimization. *Journal of Advances in Modeling Earth Systems*, 10(6), 1337–1356. <https://doi.org/10.1002/2017ms001134>
- Lu, D., Ricciuto, D., Walker, A., Safta, C., & Munger, W. (2017). Bayesian calibration of terrestrial ecosystem models: A study of advanced Markov chain Monte Carlo methods. *Biogeosciences*, 14(18), 4295–4314. <https://doi.org/10.5194/bg-14-4295-2017>
- Ma, S., Jiang, J., Huang, Y., Shi, Z., Wilson, R. M., Ricciuto, D., et al. (2017). Data-constrained projections of methane fluxes in a northern Minnesota peatland in response to elevated CO<sub>2</sub> and warming. *Journal of Geophysical Research: Biogeosciences*, 122(11), 2841–2861. <https://doi.org/10.1002/2017jg003932>
- Martens, C. S., Albert, D. B., & Alperin, M. J. (1998). Biogeochemical processes controlling methane in gassy coastal sediments—Part 1, A model coupling organic matter flux to gas production, oxidation and transport. *Continental Shelf Research*, 18, 1741–1770. [https://doi.org/10.1016/s0278-4343\(98\)00056-9](https://doi.org/10.1016/s0278-4343(98)00056-9)
- McEwing, K. R., Fisher, J. P., & Zona, D. (2015). Environmental and vegetation controls on the spatial variability of CH<sub>4</sub> emission from wet-sedge and tussock tundra ecosystems in the Arctic. *Plant and Soil*, 388(1–2), 37–52. <https://doi.org/10.1007/s11104-014-2377-1>
- Melton, J. R., Wania, R., Hodson, E. L., Poulter, B., Ringeval, B., Spahni, R., et al. (2013). Present state of global wetland extent and wetland methane modelling: Conclusions from a model inter-comparison project (WETCHIMP). *Biogeosciences*, 10, 753–788. <https://doi.org/10.5194/bg-10-753-2013>
- Mer, J. L., & Roger, P. (2001). Production, oxidation, emission and consumption of methane by soils: A review. *European Journal of Soil Biology*, 37, 25–50. [https://doi.org/10.1016/s1164-5563\(01\)01067-6](https://doi.org/10.1016/s1164-5563(01)01067-6)
- Neubauer, S. C., & Megonigal, J. P. (2015). Moving beyond global warming potentials to quantify the climatic role of ecosystems. *Ecosystems*, 18, 1000–1013. <https://doi.org/10.1007/s10021-015-9879-4>
- Nichols, J. E., & Peteet, D. M. (2019). Rapid expansion of northern peatlands and doubled estimate of carbon storage. *Nature Geoscience*, 12, 917–921. <https://doi.org/10.1038/s41561-019-0454-z>
- Nisbet, E. G., Manning, M. R., Dlugokencky, E. J., Fisher, R. E., Lowry, D., Michel, S. E., et al. (2019). Very strong. Atmospheric methane growth in the 4 years 2014–2017: Implications for the Paris agreement. *Global Biogeochemical Cycles*, 33(3), 318–342. <https://doi.org/10.1029/2018gb006009>
- Norby, R., & Childs, J. (2018). *SPRUCe: Sphagnum productivity and community composition in the SPRUCe experimental plots*. Oak Ridge National Laboratory, U.S. Department of Energy. <https://doi.org/10.25581/spruce.049/1426474>
- Norby, R., Childs, J., Hanson, P. J., & Warren, J. M. (2019). Rapid loss of an ecosystem engineer: *Sphagnum* decline in an experimentally warmed bog. *Ecology and Evolution*, 9(22), 12571–12585. <https://doi.org/10.1002/ece3.5722>
- Oleson, K., Lawrence, D. M., Bonan, G. B., Drewniak, B., Huang, M., Koven, C. D., et al. (2013). *Technical description of version 4.5 of the community land model (CLM)*. NCAR.
- Parsekian, A. D., Slater, L., Ntarlagiannis, D., Nolan, J., Sebesteyen, S. D., Kolka, R. K., & Hanson, P. J. (2012). Uncertainty in peat volume and soil carbon estimated using ground-penetrating radar and probing. *Soil Science Society of America Journal*, 76(5), 1911–1918. <https://doi.org/10.2136/sssaj2012.0040>
- Perala, D. A., & Verry, E. S. (2011). Forest management practices and silviculture. In R. Kolka, S. D. Sebesteyen, E. S. Verry, & K. N. Brooks (Eds.), *Peatland biogeochemistry and watershed hydrology at the Marcell Experimental Forest* (pp. 371–400). CRC Press. <https://doi.org/10.1201/b10708-19>
- Poulter, B., Bousquet, P., Canadell, J. G., Ciais, P., Peregon, A., Saunois, M., et al. (2017). Global wetland contribution to 2000–2012 atmospheric methane growth rate dynamics. *Environmental Research Letters*, 12(9), 094013. <https://doi.org/10.1088/1748-9326/aa8391>
- Prairie, Y., & del Giorgio, P. (2013). A new pathway of freshwater methane emissions and the putative importance of microbubbles. *Inland Waters*, 3, 311–320. <https://doi.org/10.5268/iw-3.3.542>



- Ricciuto, D., Sargsyan, K., & Thornton, P. (2018). The impact of parametric uncertainties on biogeochemistry in the E3SM land model. *Journal of Advances in Modeling Earth Systems*, *10*(2), 297–319. <https://doi.org/10.1002/2017ms000962>
- Richardson, A. D., Hufkens, K., Milliman, T., Aubrecht, D. M., Furze, M. E., Seyednasrollah, B., et al. (2018). Ecosystem warming extends vegetation activity but heightens vulnerability to cold temperatures. *Nature*, *560*(7718), 368–371. <https://doi.org/10.1038/s41586-018-0399-1>
- Rigby, M., Prinn, R. G., Fraser, P. J., Simmonds, P. G., Langenfelds, R. L., Huang, J., et al. (2008). Renewed growth of atmospheric methane. *Geophysical Research Letters*, *35*(L22805). <https://doi.org/10.1029/2008GL036037>
- Riley, W. J., Subin, Z. M., Lawrence, D. M., Swenson, S. C., Torn, M. S., Meng, L., et al. (2011). Barriers to predicting changes in global terrestrial methane fluxes: Analyses using CLM4Me, a methane biogeochemistry model integrated in CESM. *Biogeosciences*, *8*, 1925–1953. <https://doi.org/10.5194/bg-8-1925-2011>
- Sargsyan, K., Safta, C., Najm, H. N., Debusschere, B. J., Ricciuto, D., & Thornton, P. (2014). Dimensionality reduction for complex models via bayesian compressive sensing. *International Journal for Uncertainty Quantification*, *4*(1), 63–93.
- Sebestyen, S. D., Dorrance, C., Olson, D. M., Verry, E. S., Kolka, R. K., Elling, A. E., & Kyllander, R. (2011). Long-term monitoring sites and trends at the Marcell experimental fForest. In R. Kolka, S. D. Sebestyen, E. S. Verry, & K. N. Brooks (Eds.), *Peatland biogeochemistry and watershed hydrology at the Marcell Experimental Forest* (Vol. 1, pp. 15–71). CRC Press. <https://doi.org/10.1201/b10708-3>
- Segers, R., & Kengen, S. W. M. (1998). Methane production as a function of anaerobic carbon mineralization: A process model. *Soil Biology and Biochemistry*, *30*(8/9), 1107–1117. [https://doi.org/10.1016/s0038-0717\(97\)00198-3](https://doi.org/10.1016/s0038-0717(97)00198-3)
- Shi, X., Ricciuto, D. M., Thornton, P. E., Xu, X., Yuan, F., Norby, R. J., et al. (2020). Modeling the hydrology and physiology of *Sphagnum* moss in a northern temperate bog. *Biogeosciences*. <https://doi.org/10.5194/bg-2020-90>
- Shi, X., Thornton, P. E., Ricciuto, D. M., Hanson, P. J., Mao, J., Sebestyen, S. D., et al. (2015). Representing northern peatland microtopography and hydrology within the Community Land Model. *Biogeosciences*, *12*(21), 6463–6477. <https://doi.org/10.5194/bg-12-6463-2015>
- Sulman, B. N., Desai, A. R., Schroeder, N. M., Ricciuto, D., Barr, A., Richardson, A. D., et al. (2012). Impact of hydrological variations on modeling of peatland CO<sub>2</sub> fluxes: Results from the North American Carbon Program site synthesis. *Journal of Geophysical Research*, *117*. <https://doi.org/10.1029/2011JG001862>
- Sun, J., Xu, W., & Feng, B. (2004). A global search strategy of quantum-behaved particle swarm optimization. Paper presented at the *IEEE Conference on Cybernetics and Intelligent Systems*.
- Tfaily, M. M., Cooper, W. T., Kostka, J. E., Chanton, P. R., Schadt, C. W., Hanson, P. J., et al. (2014). Organic matter transformation in the peat column at Marcell Experimental Forest: Humification and vertical stratification. *Journal of Geophysical Research: Biogeosciences*, *119*, 661–675. <https://doi.org/10.1002/2013jg002492>
- Thauer, R. K., Kaster, A.-K., Seedorf, H., Buckel, W., & Hedderich, R. (2008). Methanogenic archaea: Ecologically relevant differences in energy conservation. *Nature Reviews Microbiology*, *6*(8), 579–591. <https://doi.org/10.1038/nrmicro1931>
- Thauer, R., Zinkhan, D., & Spormann, A. (1989). Biochemistry of acetate catabolism in anaerobic chemotrophic bacteria. *Annual Reviews in Microbiology*, *43*(1), 43–67. <https://doi.org/10.1146/annurev.mi.43.100189.000355>
- Thornton, P. E., Lamarque, J. F., Rosenbloom, N. A., & Mahowald, N. M. (2007). Influence of carbon-nitrogen cycle coupling on land model response to CO<sub>2</sub> fertilization and climate variability. *Global Biogeochemical Cycles*, *21*(4), GB4018. <https://doi.org/10.1029/2006gb002868>
- Thornton, P. E., & Rosenbloom, N. A. (2005). Ecosystem model spin-up: Estimating steady state conditions in a coupled terrestrial carbon and nitrogen cycle model. *Ecological Modelling*, *189*, 25–48. <https://doi.org/10.1016/j.ecolmod.2005.04.008>
- Tian, H., Xu, X., Liu, M., Ren, W., Zhang, C., Chen, G., & Lu, C. (2010). Spatial and temporal patterns of CH<sub>4</sub> and N<sub>2</sub>O fluxes in terrestrial ecosystems of North America during 1979–2008: Application of a global biogeochemistry model. *Biogeosciences*, *7*(9), 2673–2694. <https://doi.org/10.5194/bg-7-2673-2010>
- Tokida, T., Miyazaki, T., Mizoguchi, M., Nagata, O., Takakai, F., Kagemoto, A., & Hatano, R. (2007). Falling atmospheric pressure as a trigger for methane ebullition from peatland. *Global Biogeochemical Cycles*, *21*(2). <https://doi.org/10.1029/2006gb002790>
- Turetsky, M. R., Kotowska, A., Bubier, J., Dise, N. B., Crill, P., Hornibrook, E. R., et al. (2014). A synthesis of methane emissions from 71 northern, temperate, and subtropical wetlands. *Global Change Biology*, *20*(7), 2183–2197. <https://doi.org/10.1111/gcb.12580>
- Verry, E., Brooks, K., Nichols, D., Ferris, D., & Sebestyen, S. (2011). Watershed hydrology. In R. Kolka, S. D. Sebestyen, E. S. Verry, & K. N. Brooks (Eds.), *Peatland biogeochemistry and watershed hydrology at the Marcell Experimental Forest* (pp. 193–212). CRC Press
- Waddington, J., Morris, P., Kettridge, N., Granath, G., Thompson, D., & Moore, P. (2015). Hydrological feedbacks in northern peatlands. *Ecology*, *96*(1), 113–127. <https://doi.org/10.1002/ecco.1493>
- Walker, A. P., Carter, K. R., Gu, L., Hanson, P. J., Malhotra, A., Norby, R. J., et al. (2017). Biophysical drivers of seasonal variability in *Sphagnum* gross primary production in a northern temperate bog. *Journal of Geophysical Research: Biogeosciences*, *122*(5), 1078–1097. <https://doi.org/10.1002/2016jg003711>
- Walter, B. P., & Heimann, M. (2000). A process-based, climate-sensitive model to derive methane emissions from natural wetlands: Application to five wetland sites, sensitivity to model parameters, and climate. *Global Biogeochemical Cycles*, *14*(3), 745–765. <https://doi.org/10.1029/1999gb001204>
- Wang, Y., Yuan, F., Yuan, F., Gu, B., Hahn, M. S., Torn, M. S., et al. (2019). Mechanistic modeling of microtopographic impact on CH<sub>4</sub> processes in an Alaskan tundra ecosystem using the CLM-Microbe model. *Journal of Advances in Modeling Earth Systems*, *11*, 4228–4304. <https://doi.org/10.1029/2019MS001771>
- Ward, S. E., Ostle, N. J., Oakley, S., Quirk, H., Henrys, P. A., & Bardgett, R. D. (2013). Warming effects on greenhouse gas fluxes in peatlands are modulated by vegetation composition. *Ecology Letters*, *16*(10), 1285–1293. <https://doi.org/10.1111/ele.12167>
- Whiting, G. J., & Chanton, J. P. (1993). Primary production control of methane emission from wetlands. *Nature*, *364*(6440), 794–795. <https://doi.org/10.1038/364794a0>
- Xu, X., Elias, D. A., Graham, D. E., Phelps, T. J., Carrol, S. L., Wullschleger, S. D., & Thornton, P. E. (2015). A microbial functional group based module for simulating methane production and consumption: Application to an incubation permafrost soil. *Journal of Geophysical Research: Biogeosciences*, *120*(6), 1315–1333. <https://doi.org/10.1002/2015jg002935>
- Xu, X., Schimel, J. P., Thornton, P. E., Song, X., Yuan, F., & Goswami, S. (2014). Substrate and environmental controls on microbial assimilation of soil organic carbon: A framework for Earth system models. *Ecology Letters*, *17*(5), 547–555. <https://doi.org/10.1111/ele.12254>
- Xu, X., & Tian, H. (2012). Methane exchange between marshland and the atmosphere over China during 1949–2008. *Global Biogeochemical Cycles*, *26*, GB2006. <https://doi.org/10.1029/2010GB003946>
- Xu, X., Yuan, F., Hanson, P. J., Wullschleger, S. D., Thornton, P. E., Riley, W. J., et al. (2016). Review and synthesis: Four decades of modeling methane cycling within terrestrial ecosystems. *Biogeosciences*, *13*, 3735–3755. <https://doi.org/10.5194/bg-13-3735-2016>
- Ye, R., Jin, Q., Bohannan, B., Keller, J. K., & Bridgham, S. D. (2014). Homoacetogenesis: A potentially underappreciated carbon pathway in peatlands. *Soil Biology and Biochemistry*, *68*, 385–391. <https://doi.org/10.1016/j.soilbio.2013.10.020>

- Yu, Z. (2012). Northern peatland carbon stocks and dynamics: A review. *Biogeosciences*, 9, 4071–4085. <https://doi.org/10.5194/bg-9-4071-2012>
- Yuan, F., Wang, Y., Ricciuto, D. M., Shi, X., Yuan, F., Hanson, P. J., et al. (2021). An integrative model for soil biogeochemistry and methane processes: II. Warming and elevated CO<sub>2</sub> effects on peatland CH<sub>4</sub> emissions. *Journal of Geophysical Research: Biogeosciences*. <https://doi.org/10.1029/2020JG005963>
- Zalman, C., Keller, J., Tfaily, M., Kolton, M., Pfeifer-Meister, L., Wilson, R., et al. (2018). Small differences in ombrotrophy control regional-scale variation in methane cycling among Sphagnum-dominated peatlands. *Biogeochemistry*, 139(2), 155–177. <https://doi.org/10.1007/s10533-018-0460-z>
- Zhuang, Q., Melillo, J. M., Kicklighter, D. W., Prinn, R. G., McGuire, A. D., Steudler, P. A., et al. (2004). Methane fluxes between terrestrial ecosystems and the atmosphere at northern high latitudes during the past century: A retrospective analysis with a process-based biogeochemistry model. *Global Biogeochemical Cycles*, 18(3), GB3010. <https://doi.org/10.1029/2004GB002239>
- Zona, D., Oechel, W. C., Kochendorfer, J., Paw U, K. T., Salyuk, A., Olivas, P., et al. (2009). Methane fluxes during the initiation of a large-scale water table manipulation experiment in the Alaskan Arctic tundra. *Global Biogeochemical Cycles*, 23. <https://doi.org/10.1029/2009gb003487>

### Reference From the Supporting Information

- Cao, M. K., Dent, J. B., & Heal, O. W. (1995). Modeling methane emissions from rice paddies. *Global Biogeochemical Cycles*, 9(2), 183–195. <https://doi.org/10.1029/94gb03231>